Pichler, Thomas ; Veizer, Jan ; Hall, Gwendy E.M

The chemical composition of shallow-water hydrothermal fluids in Tutum Bay, Ambitle Island, Papua New Guinea and their effect on ambient seawater

Journal Article as: peer-reviewed accepted version (Postprint)

DOI of this document*(secondary publication): https://doi.org/10.26092/elib/3255

Publication date of this document: 02/12/2024

* for better findability or for reliable citation

Recommended Citation (primary publication/Version of Record) incl. DOI:

Thomas Pichler, Jan Veizer, Gwendy E.M Hall, The chemical composition of shallow-water hydrothermal fluids in Tutum Bay, Ambitle Island, Papua New Guinea and their effect on ambient seawater, Marine Chemistry, Volume 64, Issue 3, 1999, Pages 229-252, ISSN 0304-4203, https://doi.org/10.1016/S0304-4203(98)00076-0.

The chemical composition of shallow-water hydrothermal fluids in Tutum Bay, Ambitle Island, Papua New Guinea and their effect on ambient seawater

Thomas Pichler [a,*], Jan Veizer [a,b], Gwendy E.M. Hall [c]

[a] *Ottawa-Carleton Geoscience Centre, University of Ottawa, Ottawa, Ontario, Canada, K1N 6N5*
[b] *Institut fuer Geologie, Ruhr Universitaet, 44780 Bochum, Germany*
[c] *Geological Survey of Canada, 601 Booth Street, Ottawa, Ontario, Canada, K1A 0E8*

---

[*] Corresponding author. Tel.: +1-613-562-5800 ext. 6639; Fax: +1-613-562-5192; E-mail: tpichler@nrcan.gc.ca

1. Introduction

The chemical composition of seawater is controlled through the combined effort of numerous processes, such as low and high temperature seafloor alteration, fluvial and atmospheric input, and sedimentation. Most studies of seafloor hydrothermal activity have focused primarily on deep-sea, hydrothermal systems found along volcanically active portions of the mid-ocean ridges or in deep back-arc basins. Submarine hydrothermal activity and hydrothermal alteration of oceanic crust, however, is not confined to deep-water environments. Additional locations are found in much shallower water at the flanks of volcanic islands and on the tops of seamounts (e.g., Vidal et al., 1978; Vidal et al., 1981; Sarano et al., 1989; Butterfield et al., 1990; Varnavas and Cronan, 1991; Dando and Leahy, 1993; Hodkinson et al., 1994; Pichler et al., 1995; Heikoop et al., 1996; Sedwick and Stüben, 1996). The submerged flanks of island arc volcanoes provide an exceptional opportunity to study the essential differences and similarities between subaerial and submarine venting and the transition from one to the other.

Here we report on the chemistry of shallow-water hydrothermal fluids in Tutum Bay and their effect on ambient seawater composition. In this near-shore, shallow-water setting, physicochemical conditions may not be drastically different from on-shore hydrothermal systems, for example, in terms of pressure and temperature, but their discharge into seawater sets them apart. Mixing with cold oxidizing seawater provides a mechanism for precipitation of dissolved constituents in the hydrothermal fluids. Mixing may occur right at the seawater±seafloor interface for an impermeable seafloor, or in the subsurface if local sediments are saturated with seawater. As a result, Eh, pH and temperature change in the hydrothermal fluid, in pore water and in ambient seawater.

2. Location and geological setting

Our study area lies along the southwest margin of Ambitle Island, one of the Feni islands in the southernmost island group of the Tabar±Feni chain, Papua New Guinea (Fig. 1). The islands of the Tabar±Feni

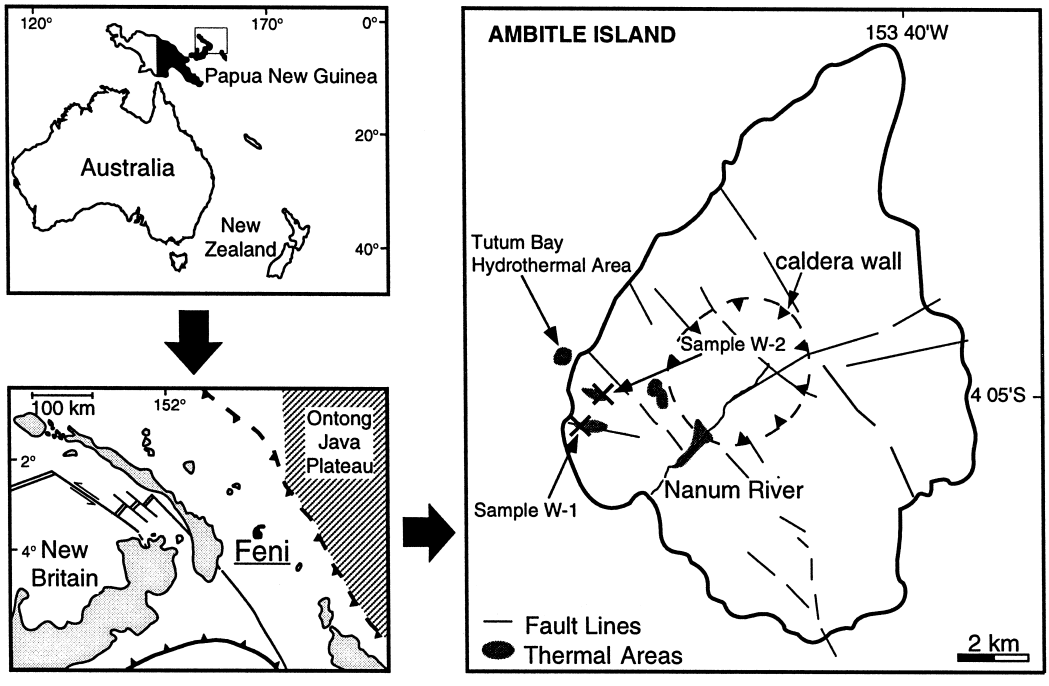

Fig. 1. Location of Ambitle Island, one of the Feni islands in eastern Papua New Guinea (modified after Licence et al., 1987 and Pichler and Dix, 1996). Geothermal areas indicated in dark are primarily along the western side of the island.

chain are Pliocene-to-Recent alkaline volcanoes that occur in the forearc region of the former ensimatic New Hanover±New Ireland±Bougainville island arc (Fig. 1). The volcanoes erupt an unusual suite of silica-undersaturated, high-K calc-alkaline lavas generated by adiabatic decompression melting during the uplift of the New Ireland forearc basin (McInnes and Cameron, 1994). The Tabar±Feni volcanoes stand apart from the surrounding arc volcanoes of New Ireland and New Britain in that they have a proclivity towards producing Au mineralization as epitomized by the world-class Ladolam Au deposit (40 million oz) on Lihir island (Davies and Ballantyne, 1987).

Ambitle Island is part of a Quaternary stratovolcano with a central eroded caldera built on poorly exposed Oligocene marine limestone (Wallace et al., 1983). Volcanic strata (interbedded lava flows, lahar deposits, tuffs, and scoriae) dip radially from the island, presumably extending beneath the shelf. Several geothermal areas are located primarily along the western coast and in the western part of the caldera near breaches in the caldera wall (Fig. 1). Hot mud pools, springs of chloride and acid sulfate waters, and a few low temperature fumaroles are present, with temperature and pH values ranging from 67 to 100°C and 1.9 to 9.1, respectively (Wallace et al., 1983).

3. Field observations

Submarine, hydrothermal venting occurs at Tutum Bay (Figs. 1 and 2) in shallow (5±10 m) water along the inner shelf that contains a patchy distribution of coral±algal reefs surrounded by medium to coarse-grained mixed carbonate±volcaniclastic sand and gravel. The site is located along a fault trace that intersects several of the on-land geothermal areas (Fig. 1).

Two types of venting are observed. (1) Focused discharge of a clear, two-phase fluid occurs at dis-

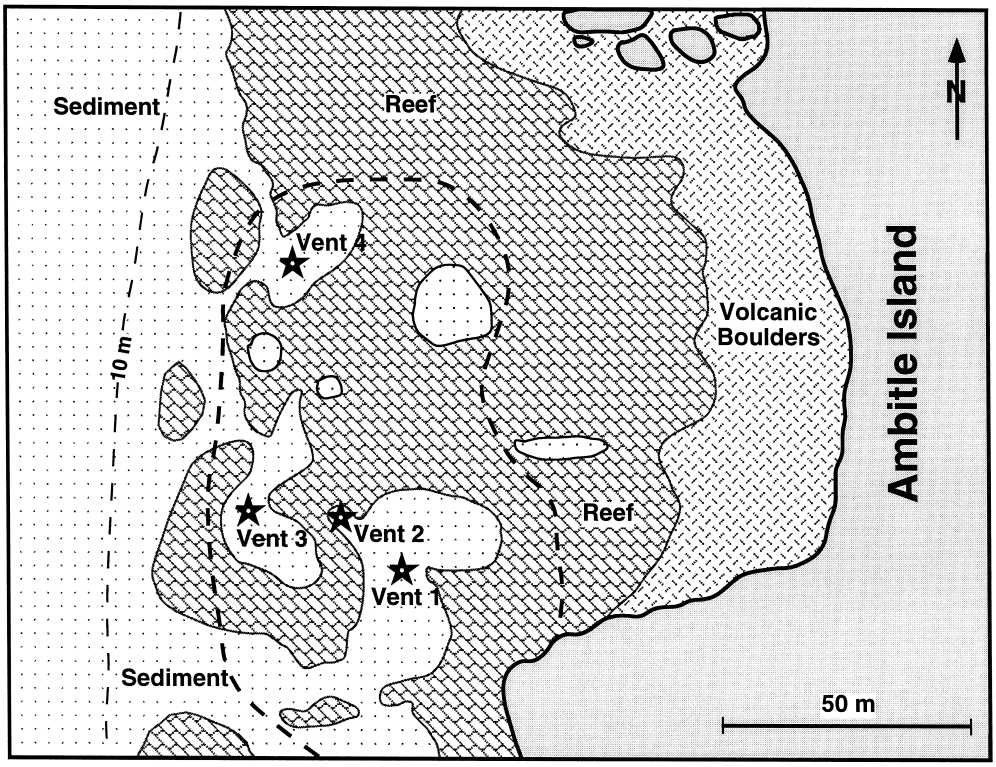

Fig. 2. Location of hydrothermal vents within Tutum Bay on the west side of Ambitle Island. The bold dashed line indicates the extent of gaseous discharge.

Fig. 3. Underwater photographs of focused discharge in Tutum Bay. (a) Vent 1 and (b) Vent 3. The field of view is ~ 18 m at a water depth of 8 m for (a).

crete ports, 10±15 cm in diameter, with minor phase separation (boiling) at the sea floor. There is no associated topographic edifice. This type of discharge produces a roaring sound underwater and has an estimated flow rate as high as 300 to 400 l/min (i.e., fire hose). Shimmering and a whitish coloration, indicative of hot water and water vapor, extends several meters above vent portals (Fig. 3a). Fluid temperatures at portal entrances are between 89 and 98°C. (2) Dispersed or diffuse discharge consists of streams of gas bubbles (> 95% CO_2) emerging directly through the sandy to pebbly unconsolidated sediment and through fractures in volcanic rocks (Fig. 4). This type of venting appears to be itinerant, with shifts in locations on the order of tens of centimeters, possibly related to tortuous migration through the surface sediment.

Gases that discharge through unconsolidated sediment often carry an equivalent amount of water with them. The sediment cover in Tutum Bay, however, is very thin (10±30 cm) which does not allow for an extensive gas seep induced interstitial water circulation. This is in contrast to other areas of gas discharge where sediment covers are thicker (e.g., O'Hara et al., 1994). As a result, there is clear separation between liquid and gaseous discharges in Tutum Bay.

Four locations of focused venting are present in Tutum Bay (Fig. 2). Vents 1 and 2 are single vents with hydrothermal discharge from only one orifice (Fig. 3a) and vent 3 is an assemblage of three vents that are very close together in an area of approximately 2×2 m^2 (Fig. 3b). Vent 4 is located some distance north of the other three vents (Fig. 2) and it is closely associated with an area of massive gas emanation (Fig. 4). Vent 4 is slightly different from the other vents; here shimmering hot water discharges at low rates through several small orifices (1 to 5 cm é) in an area of approximately 1×3 m^2. Based on their geographic position, the vents have been divided into two groups, A and B; area A consists of vents 1, 2 and 3 and area B of vent 4 (Fig. 2).

Hydrothermal precipitates accumulate on dead coral substrate and rock fragments surrounding vent portals and include euhedral aragonite crystals and

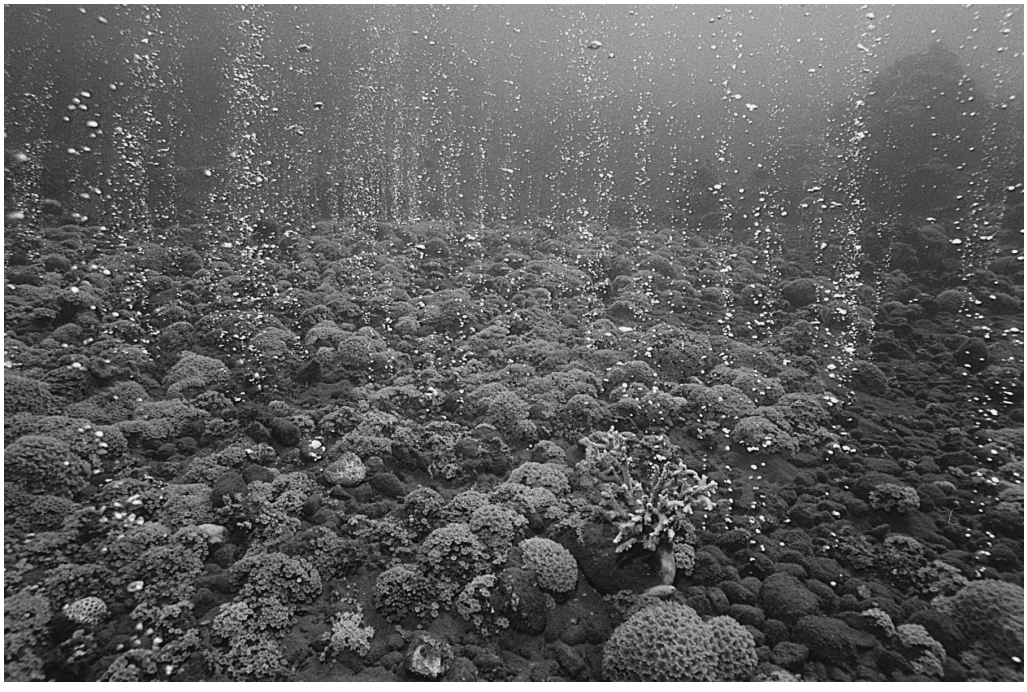

Fig. 4. Underwater photograph of the diffuse gaseous discharge around vent 4. The field of view is ~ 8 m at a water depth of 9 m.

microcrystalline crusts of Fe-oxyhydroxide, aragonite, and ferroan calcite (Pichler and Dix, 1996).

Two of the on-shore hot springs, Waramung and Kapkai were sampled in addition to the Tutum Bay vents for comparison. A detailed description of these sites can be found elsewhere (Wallace et al., 1983; Licence et al., 1987).

4. Sampling and analytical procedures

Generally the chemical analysis of water samples is more accurate under well-controlled laboratory conditions than in the field. Some parameters, however, are unstable and, therefore, must be measured immediately after sampling. In this study we used sample containers, preservation techniques and holding times recommended for water analysis by the US Federal Registry (HACH, 1992). Vent temperatures were measured with a maximum thermometer. Due to inherent difficulties when working underwater, however, these measurements should be regarded as minimum temperatures. Vent samples were collected over a period of 10 days either by inserting a Teflon® tube as far as possible into the vent orifice or covering the vent orifice with a Teflon® funnel. Sixty-milliliter medical syringes were connected to the Teflon tube or funnel via a three-way stopcock. Using this set-up, generally 15 syringes were filled at a time and brought to the surface. While sampling vents 2, 3 and 4 minor amounts of water vapor, indicative of phase separation, were observed during filling of the syringes. On-board, aliquots were taken and immediately analyzed for pH, conductivity and alkalinity. Total alkalinity (A^T) was measured as equivalent $CaCO_3$ and expressed as HCO_3^-, using a Hach digital titrator and titrating to an endpoint of pH 4.5 (HACH, 1992). The remaining solution was filtered to < 0.45 μm and subsequently separated into subsets for later analyses. Samples were stored in high density polyethylene bottles and aliquots for cation and trace element analyses were acidified with ultrapure HNO_3. Additionally, 60 ml aliquots of selected samples were acidified with double distilled HCl (35%) for determination of As^{3+}/As^{5+}.

The single orifice vents 1 and 2 were sampled twice and duplicate samples are indicated by a capital letter following the sample number, i.e., 1B. Two of the three orifices at vent 3 were sampled, i.e., 3-1 and 3-2. A duplicate of 3-1 was taken. At vent 4, three samples were taken from three different orifices within a single mound, i.e., 4, 4B, 4C. A sample of ambient seawater (SW) and the samples W-1 and W-2 from the on-shore hot springs were sampled by submerging a 1-l high density polyethylene bottle. These sample were treated exactly as the Tutum Bay vent waters.

Seventy-five seawater samples were collected for chemical analyses throughout the bay at the bottom, in mid-water and at the surface at varying distances from vent sites in order to reconstruct the dissipation of the hydrothermal plume and its influence on the seawater composition in Tutum Bay. Samples were pumped to the surface through a Nalgene® tube that was lowered to the depth of sampling. In order to avoid contamination, several tube volumes were discarded before taking the actual sample. Horizontal distance from vent sites was determined with ropes and buoys. At the time of sampling no water movement (current) other than that caused by the hydrothermal vents themselves was observed. These samples were filtered to < 0.45 μm, acidified with ultrapure HNO_3 for later laboratory analyses and stored in high-density polyethylene bottles.

Throughout the sampling period several samples of deionized water were treated in the same way as the vent samples, i.e., filtered, acidified and filled into high density polyethylene bottles. These samples were later analyzed together with the vent samples in order to check for possible contamination.

Major cations, trace elements, ultra trace elements and rare earth elements (REE) were determined at the Geological Survey of Canada: Li, Rb, Sr, Sb, Cs, and Tl by direct inductively coupled plasma mass spectrometry (ICP-MS) and Fe and Mn by chelation ICP-MS following a tenfold dilution with deionized water. REEs were analyzed by chelation ICP-MS without dilution. A more detailed description of the direct and chelation ICP-MS methodology and associated figures of merit can be found elsewhere (Hall et al., 1995, 1996). Ca^{2+}, Mg^{2+}, Na^+ and K^+ were measured by flame atomic absorption spectrometry (FAA). Prior to analyses for Ca^{2+}, Mg^{2+}, Na^+ and K^+, a Cs/La buffer solution was added to a suitable aliquot of the sample to suppress ionization. Si and B

Table 1
Location, temperature, pH and major element composition of Tutum Bay vent waters, ambient seawater and onshore geothermal springs in moles per kilogram

No. of unit	Location	T (°C)	pH	Cl (mmol)	Br (mmol)	SO_4 (mmol)	HCO_3 (mmol)	B (mmol)	Si (mmol)	Na (mmol)	K (mmol)	Ca (mmol)	Mg (mmol)	Li (μmol)	Mn (μmol)	Fe (μmol)	Rb (μmol)	Sr (μmol)	Cs (μmol)	Sb (μmol)	Tl (μmol)	As^{3+} (μmol)	As^{T} (μmol)
1	Vent 1	90	6.2	34	0.1	11	13	0.8	3.7	54	2.5	5.1	2.5	146	8.4	29	4.0	77	0.4	0.1	0.02	10.0	10.9
1B	Vent 1	90	6.2	35	0.1	11	13	0.7	3.7	52	2.4	5.2	2.7	145	8.1	28	3.9	76	0.4	0.1	0.02	10.7	10.7
2	Vent 2	80	6.3	66	0.1	12	13	0.8	3.4	74	2.7	5.6	5.6	135	7.9	28	3.8	79	0.4	0.1	0.02	10.3	10.4
2B	Vent 2	80	6.2	81	0.2	12	13	n.d.	3.3	83	2.8	5.7	6.6	132	7.9	26	3.7	79	0.4	0.1	0.02	9.4	9.4
3-1	Vent 3	88	6.3	87	0.1	12	13	0.7	3.3	88	2.9	5.8	7.2	127	7.7	27	3.7	80	0.4	0.1	0.02	9.2	9.2
3-1B	Vent 3	88	6.2	49	0.1	12	13	0.8	3.6	60	2.5	5.5	3.7	135	8.6	30	3.9	81	0.4	0.1	0.02	9.5	9.8
3-2	Vent 3	89	6.2	54	0.1	11	13	0.7	3.5	64	2.6	5.5	4.1	135	8.7	29	3.9	80	0.4	0.1	0.02	9.8	9.9
4	Vent 4	90	6.2	46	0.1	10	13	0.8	3.5	59	2.8	4.9	3.5	136	6.5	18	4.1	73	0.4	0.1	0.02	10.8	11.7
4B	Vent 4	90	6.4	54	0.1	11	14	0.8	3.5	63	3.1	5.0	4.1	134	6.4	17	4.1	73	0.4	0.1	0.02	10.1	11.1
4C	Vent 4	91	6.7	83	0.2	12	13	0.7	3.2	84	3.2	5.3	6.6	125	6.1	17	3.9	74	0.4	0.1	0.02	9.6	11.8
W-1	Waramung Hot Spring	98	8.8	337	0.4	66	9.2[a]	4.1	3.0	420	36	0.2	0.04	619	0.04	0.4	32.4	24	3.4	1.3	0.10	20.7	20.7
W-2	Kapkai Hot Spring	92	8.4	390	0.3	74	11[a]	5.1	3.7	490	40	0.1	0.03	732	0.03	0.4	39.1	30	4.1	0.3	0.08	38.8	38.8
SW	Seawater	28	8.0	548	0.6	29	2.5	0.4	0.0	450	9.1	10.1	50.8	20	0.03	0.3	1.2	91	0.004	0.004	0.001	n.d.	0.05

n.d. = Not determined.
[a]Values represent total alkalinity because they include HS^- alkalinity.
Repeat standard deviations in % are as follows: Cl, Br, SO_4, B, Si, Na, Ca, Fe, Mn, Rb, Sr, < 5%; K = 7%; Sb = 16%; As = 17%.

were analyzed by ICP-ES. The total arsenic (As^T) concentration was measured by AAS at a solution pH < 2 as As-hydride and As^{3+} was determined by AAS as As^{3+}-hydride, generated at pH 5 (citrate buffer) (Driehaus and Jekel, 1992). Finally, As^{5+} was calculated from the difference between As^T and As^{3+}. Anion (Cl^-, Br^-, SO_4^{2-}) concentrations were measured at the University of Ottawa with a Dionex 100 High Pressure Liquid Chromatograph. Calibration curves were constructed using a control blank and DIONEX standard solutions. The overall completeness and quality of each analyses was checked by performing a charge balance according to: Σanions (meq) = Σcations (meq). The difference was always less than 5%.

Gas samples were collected into 600-ml bottles through an inverted Teflon® funnel that was placed over the vent. In order to estimate the total gas flux from Tutum Bay, more than 100 flux measurements were carried out by timing the replacement of a known water volume from a graded cylinder. All flux measurements were normalized to 1 bar (i.e., atmospheric pressure at sea level). The chemical composition was analyzed at the Institute of Geological and Nuclear Sciences in Lower Hutt, New Zealand following Giggenbach and Goguel (1989).

5. Results

5.1. General statement

The samples collected from the submarine vents in Tutum Bay are mixtures of hydrothermal fluid and seawater (Table 1). Entrainment of ambient cool seawater may have happened in the shallow seafloor or during sampling. Assuming conservative behavior during mixing, several chemical species can be used to trace the mixing process if the concentration difference between seawater and hydrothermal fluid is sufficient. The best case scenario is if the element under consideration is absent in one of the mixing partners. The early laboratory study of Bishoff and Dickson (1975) showed that high temperature (> 200°C) hydrothermal fluids have lost all their Mg due to precipitation of Mg-rich minerals in the subsurface. Although the fluids that was discharged in Tutum Bay are quite different from those studied by

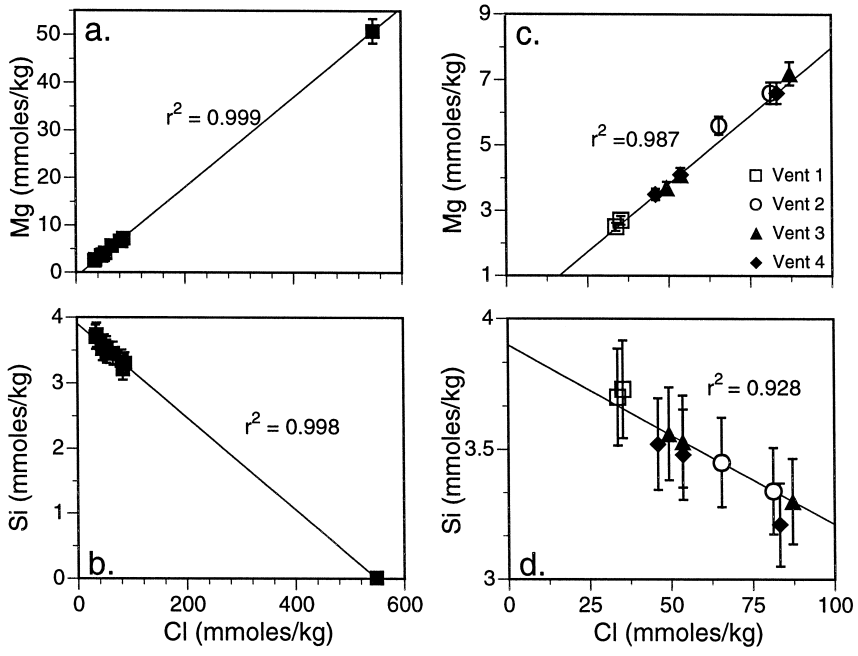

Fig. 5. (a) Dissolved Mg vs. Cl in Tutum Bay vent waters and seawater. (b) Dissolved Si vs. Cl in Tutum Bay vent waters and seawater. (c) Dissolved Mg vs. Cl for individual vents. (d) Dissolved Si vs. Cl for individual vents.

Table 2
Calculated endmember composition for pH, major and selected minor elements in Tutum Bay vent waters in moles per kilogram

Sample unit	Cl (mmol)	Br (mmol)	SO_4 (mmol)	B (mmol)	Si (mmol)	Na (mmol)	K (mmol)	Ca (mmol)	Mg (mmol)	Li (μmol)	Mn (μmol)	Fe (μmol)	Rb (μmol)	Sr (μmol)	Sb (μmol)	Cs (μmol)	Tl (μmol)	As (μmol)
1	7.4	0.05	10	0.8	3.9	34	2.1	4.9	0[a]	153	8.9	30	4	76	0.1	0.5	0.02	12
1B	6.8	0.08	10	0.8	3.9	29	2.0	4.9	0[a]	152	8.6	29	4	75	0.1	0.5	0.02	11
2	6.3	0.12	10	0.8	3.9	27	2.0	5.1	0[a]	150	8.9	32	4	77	0.1	0.5	0.02	12
2B	12	0.16	9	n.d.	3.8	28	1.9	5.0	0[a]	149	9.1	29	4	78	0.1	0.5	0.02	10
3-1	11	0.06	10	0.8	3.8	28	1.8	5.1	0[a]	145	8.9	32	4	78	0.1	0.5	0.02	10
3-1B	8.1	0.09	10	0.8	3.8	29	2.0	5.1	0[a]	144	9.3	33	4	80	0.1	0.5	0.02	11
3-2	8.7	0.07	9	0.8	3.8	29	2.0	5.1	0[a]	145	9.4	32	4	79	0.1	0.5	0.02	11
4	8.8	0.09	9	0.8	3.8	29	2.4	4.5	0[a]	145	7.0	19	4	72	0.1	0.5	0.03	13
4B	10	0.10	9	0.8	3.8	29	2.5	4.5	0[a]	144	6.9	19	4	71	0.1	0.5	0.03	12
4C	11	0.21	9	0.8	3.7	29	2.3	4.5	0[a]	141	7.0	19	4	71	0.1	0.5	0.02	14

[a] Mg concentration for these samples is 0 by convention.

Bishoff and Dickson (1975), we use Mg as an indicator for seawater entrainment. Given their chemical composition and proximity to shore, our hydrothermal fluids most likely derived from meteoric waters which are already much lower in Mg when compared to seawater. In addition, most studies of deep circulating meteoric derived geothermal waters show very low concentrations of Mg (< 1 mg/l) (e.g., Nicholson, 1992) and as confirmed by our analyses of samples W-1 and W-2 (Table 1). The assumption of complete Mg absence in the vent fluids is most likely not correct, but given the enormous concentration difference between seawater and vent fluid, it is well within any analytical uncertainty. Another option to correct for seawater entrainment is to use Si as a tracer of mixing (e.g., Sedwick and Stüben, 1996). Both alternatives have been explored in Fig. 5, where we have plotted Si and Mg^{2+} vs. Cl^- with their respective linear regression fits. The Si values, although consistently decreasing with an increase of seawater component (i.e., Cl^- concentration), deviate barely beyond their analytical error (Fig. 5b,d). Relative to ambient seawater, Mg^{2+} is depleted and Si is enriched and both show almost perfect correlation ($r^2 > 0.99$) with Cl^- (Fig. 5a,b). This high correlation, however, is due to the outlier effect (Swan and Sandilands, 1995) caused by the seawater data point. Excluding this outlier (Fig. 5c,d), the correlation, although, still high, is somewhat less for Si ($r^2 = 0.928$) than for Mg^{2+} ($r^2 = 0.987$). Therefore, we assume that for our samples, Mg^{2+} is a more reliable tracer of mixing. The poorer correlation for Si may be due to its higher susceptibility to changes in temperature and its greater inclination to post-sampling concentration changes due to adsorption onto container walls.

The data presented in Table 2 are endmember compositions that have been calculated according to the following formula:

$$X_{hf} = \frac{X_m - X_{sw}(Mg_m/Mg_{sw})}{1 - (Mg_m/Mg_{sw})} \quad (1)$$

where X_{hf} is the calculated endmember concentration, X_m is the measured concentration and X_{sw} is the concentration in seawater. No correction of chemical composition for phase separation was attempted. In order to account for phase separation, the sampling pressure, steam composition and/or reservoir conditions have to be known (Henley et al., 1984). This information can generally be obtained when sampling in explored on-land geothermal systems, but not when sampling underwater hot-springs. The effect on chemical composition by phase separation in Tutum Bay vent waters, however, seems to be negligible. Only minor amounts of steam were observed while sampling vents 2, 3 and 4 and no steam

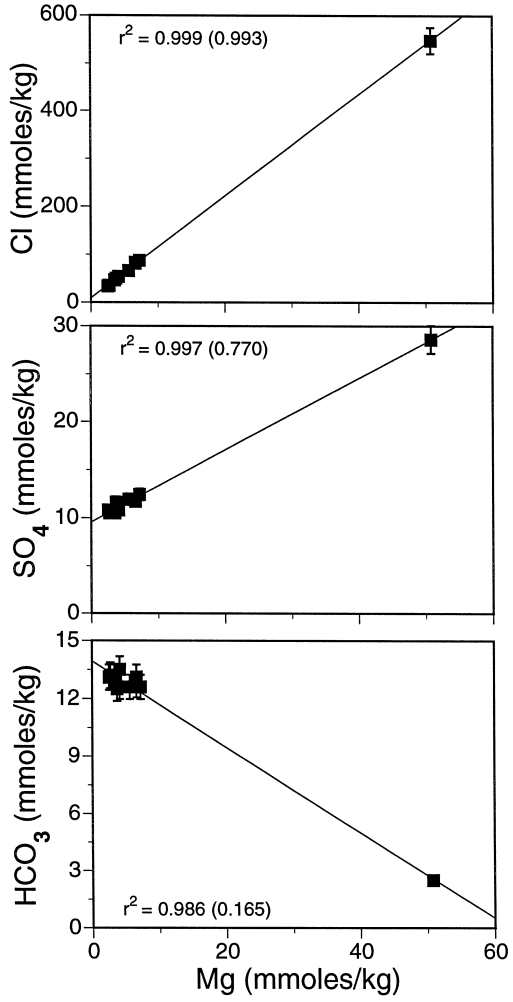

Fig. 6. Major anions (Cl, SO_4 and HCO_3) vs. Mg in Tutum Bay vent waters and seawater. r^2 is the correlation coefficient for the linear regression taking into account the whole data set including seawater (Mg ~ 51 mmol) and r^2 in brackets is the correlation coefficient for the linear regression excluding seawater. See text for more details.

was observed at vent 1. The impression of heavy boiling seems to be an effect caused by simultaneous discharge of non-condensable gas and water.

The samples, W-1 and W-2, from the on-land thermal areas were taken from the same springs as samples WA1 and KP in Licence et al. (1987). Their chemical composition is in excellent agreement, indicating stable conditions for these springs during more than 12 years.

5.2. Chemical composition of Tutum Bay vent waters

The vent waters from Tutum Bay are depleted in Br^-, SO_4^{2-} and Cl^- relative to ambient seawater and SO_4^{2-} and Cl^- are positively correlated with Mg^{2+} (Fig. 6). There are no distinct trends for individual vents; all samples either follow the same vent water±seawater mixing trend or plot in one cluster. HCO_3^- is enriched relative to ambient seawater and negatively correlated with Mg^{2+}. The linear regression analysis shows a very high degree of correlation for all three species (> 0.986), but excluding the seawater outlier the correlation for SO_4^{2-} is much less ($r^2 = 0.77$) and for HCO_3^- there is no more correlation ($r^2 = 0.165$). Endmember compositions are listed in Table 2. For all samples, SO_4^{2-} values are within their analytical uncertainty. Cl^- and Br^-, however, show a significant spread except for vent 1.

The alkaline metals Li^+, Rb^+ and Cs^+ are significantly enriched over ambient seawater and negatively correlated with Mg^{2+} (Table 1 and Fig. 7). Na^+ and K^+ are significantly depleted relative to seawater and positively correlated with Mg^{2+} (Table 1 and Fig. 7). The Na^+ depletion is similar to the depletion observed for Cl^-. Again, excluding the seawater outlier, only Na^+ maintains the high degree of correlation (Fig. 7). Endmember concentrations are listed in Table 2. Except for the Na^+ value in sample 1, which is slightly higher than the rest, all Na^+ and Li^+ analyses are within their analytical error. The K^+ values fall into two distinct groups for

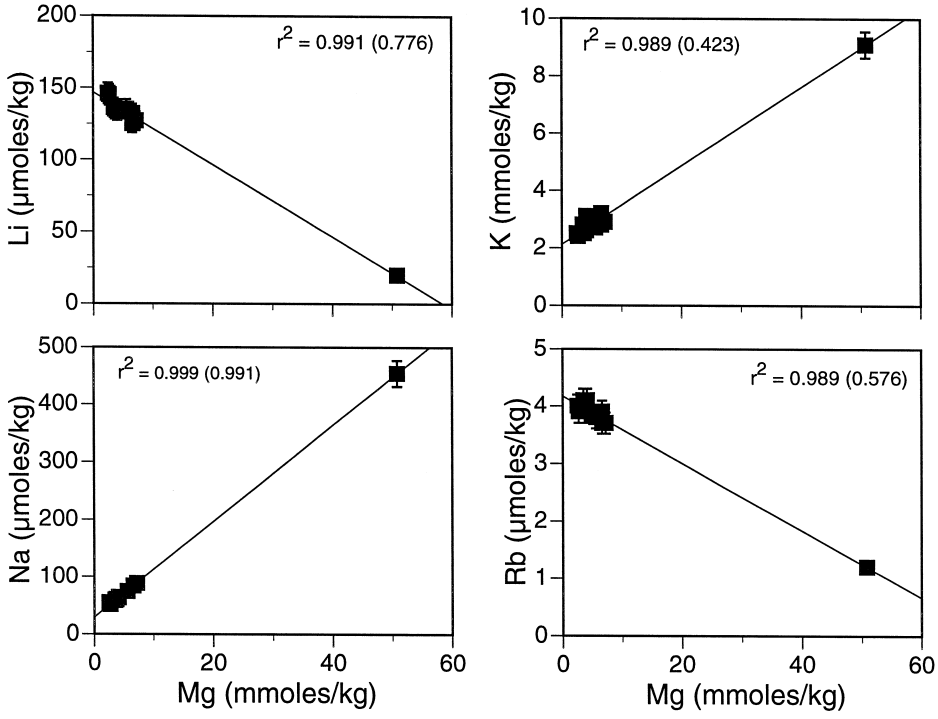

Fig. 7. Li, Na, K and Rb vs. Mg in Tutum Bay vent waters and seawater. Explanation of correlation coefficients as in Fig. 6. See text for more details.

area A and area B, with higher concentrations in B. The Rb^+ and Cs^+ concentrations are within their analytical error, the values for area B, however, are consistently higher than those for area A.

All Tutum Bay vent waters have Ca^{2+} concentrations that are significantly lower than ambient seawater (Table 1 and Fig. 8). Values for vents in area A and area B plot in two distinct groups that are both positively correlated with Mg^{2+} (Fig. 8). Linear regression analysis shows a high degree of correlation ($r^2 > 0.99$) for both groups, which is maintained ($r^2 > 0.93$) after exclusion of the seawater outlier (Fig. 8). The Sr^{2+} concentration in vent waters is only slightly lower than in ambient seawater and there is no apparent correlation between Sr^{2+} and Mg^{2+}. Endmember concentrations for both areas are within their respective analytical uncertainty, but area A vents have slightly higher values (Table 2).

The transition metals Fe and Mn are highly enriched over ambient seawater (Table 1 and Fig. 9).

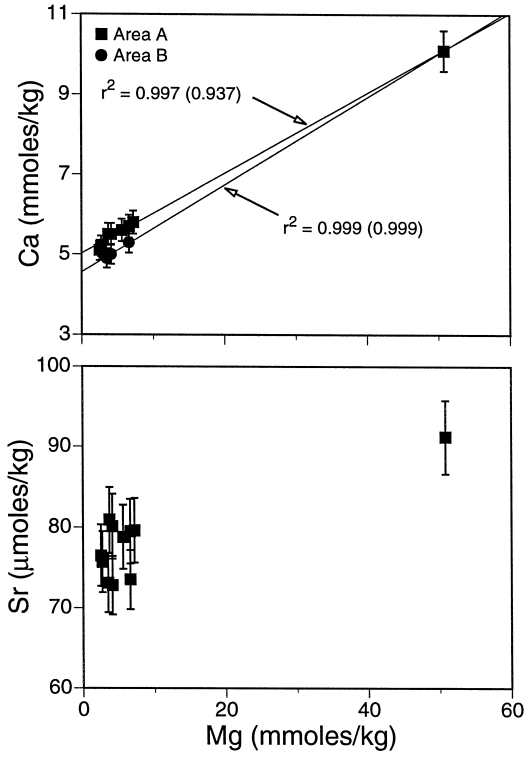

Fig. 8. Ca and Sr vs. Mg in Tutum Bay vent waters and seawater. Explanation of correlation coefficients as in Fig. 6. See text for more details.

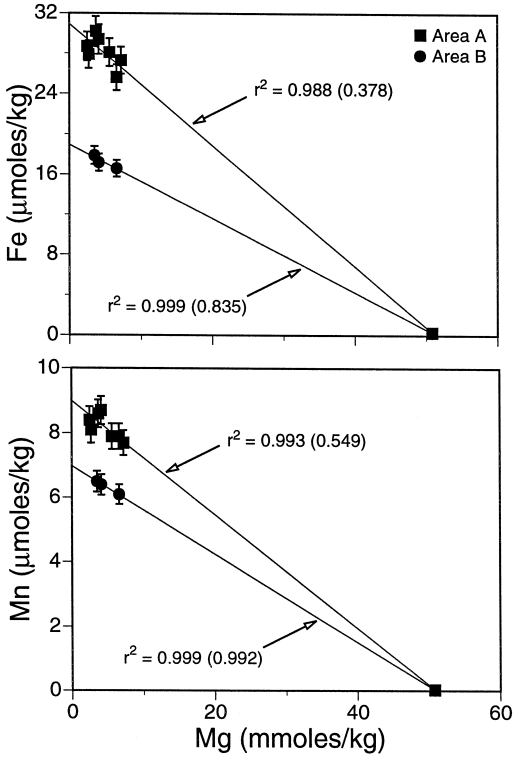

Fig. 9. Fe and Mn vs. Mg in Tutum Bay vent waters and seawater. Explanation of correlation coefficients as in Fig. 6. See text for more details.

Values for vents in area A are higher than those from area B, but both are positively correlated with Mg^{2+} (Fig. 9). After exclusion of the seawater value, correlation for area A drops substantially while for area B it remains high. The values for the individual areas, however, do not deviate beyond their analytical error. Endmember concentrations for both areas are within their respective analytical uncertainty, but area A vents have significantly higher values (Table 2).

Relative to ambient seawater, Sb, As and Tl are significantly enriched in all vents (Table 1). Arsenic concentrations are up to 275 times above seawater and it is dominantly present in its trivalent state. Endmember concentrations for Sb, As and Tl fall into groups, as observed for Ca^{2+}, Fe and Mn, except that here values for area B are higher than those for area A.

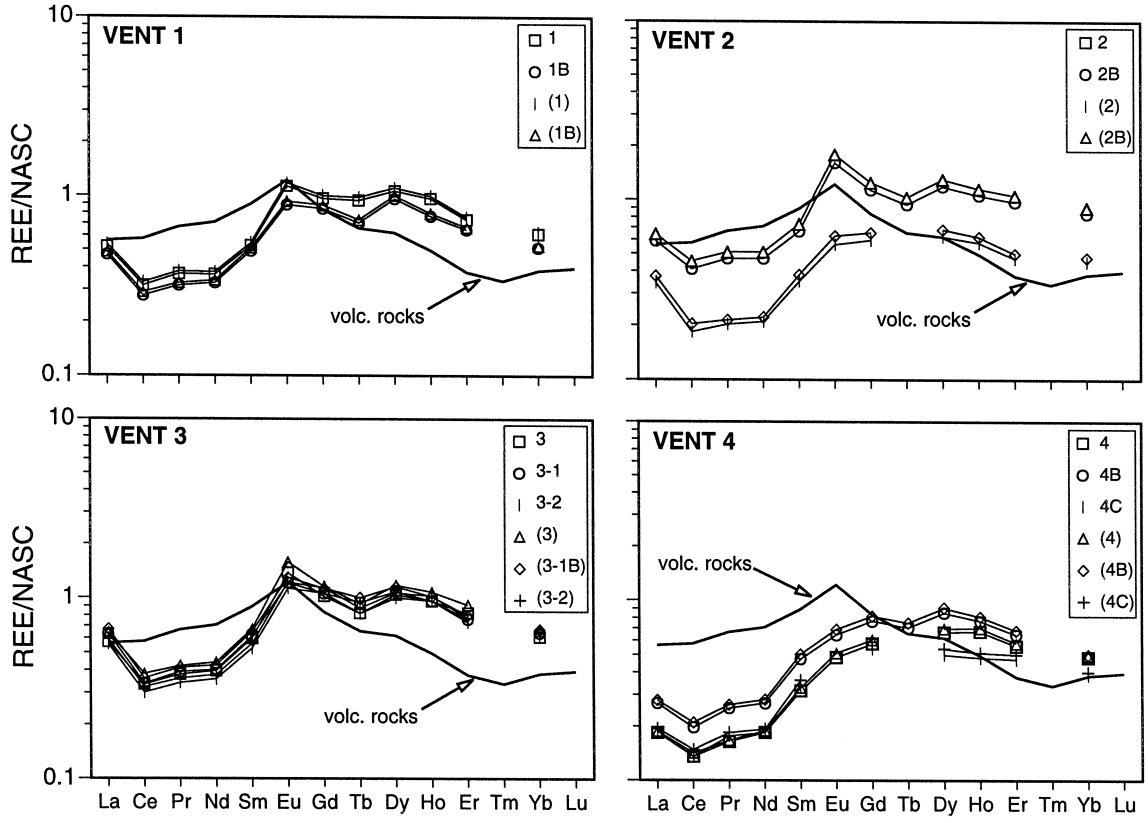

Fig. 10. North American Shale Composite (NASC) (Haskin et al., 1968) normalized rare earth element plots for vents 1, 2, 3 and 4. REE concentrations for vent waters are multiplied by 106. The bold pattern without labels represents the average REE composition of volcanic rocks from Ambitle Island; data are from Wallace et al. (1983). Raw data are available from: tpichler@nrcan.gc.ca.

REE concentrations in Tutum Bay vent waters are generally one order of magnitude higher than those reported for average seawater (Fleet, 1984). North American Shale Composite (NASC) normalized raw and endmember concentrations are plotted in Fig. 10. The pattern geometry for raw and endmember values is effectively the same, except that the endmember patterns plot slightly higher. The samples from vents 1 and 3 (1, 3-1 and 3-2) and their duplicates (1B and 3-1B) plot very closely together, showing the same pattern geometry: an initial drop from La to Ce followed by rise from the Ce minimum to an Eu maximum and a slight decrease towards an intermediate Lu. The pattern geometry for samples from vent 4 (4, 4B and 4C) is quite different; REE concentrations initially drop from La to a Ce minimum which is followed by a rise to a Dy maximum and a slight decrease towards Lu.

5.3. Gas compositions

The chemical compositions of two samples collected from submarine gas vents in Tutum Bay are listed in Table 3. In all the gases, CO_2 is the

Table 3
Chemical compositions of dry gases from Tutum Bay in mmol/mol; T (°C) is the CH_4/CO_2 equilibration temperature

Sample	CO_2	H_2S	He	H_2	O_2	N_2	N_2 (c)	CH_4	T (°C)
TB-1	927	< 0.3	0.021	< 0.01	7.3	44	29	20	257
TB-2	966	< 0.3	0.012	< 0.01	5.4	22	11	6	291
TB-3	979	< 0.3	< 0.01	< 0.01	6.1	36	24	14	268
TB-4	949	< 0.3	< 0.01	< 0.01	4.3	35	23	14	267
TB-5	926	< 0.3	0.011	< 0.01	5.8	47	35	20	257

$N_2(c) = N_2 - 2O_2$.
n.d. = Not determined.

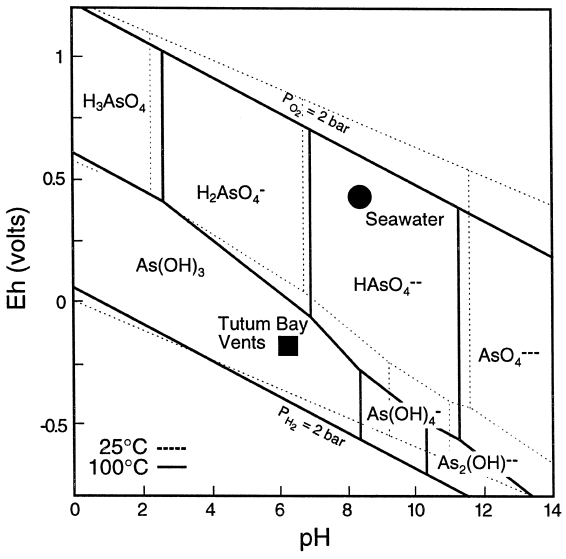

Fig. 11. Eh±pH diagram for the system As±O±H at 25°C (dashed lines) and 100°C (solid lines) at a pressure of 1.013 bars. Activities of $As(OH)_4^-$ and HCO_3^- are assumed to be 10^{-3} and 10^{-4}, respectively. Thermodynamic data are from Brookins (1988) and references therein.

dominant component and its approximate flux is 100 dm^3/s. All the submarine gases contain significant amounts of O_2, either representing an inherent component of these gases, dissolved air stripped from seawater by the rising gas bubbles, or being introduced during sampling. In the absence of any information on the origin of O_2 and N_2, their concentrations can be corrected by subtracting $2O_2$ from measured values of N_2 to obtain $N_2(c)$ (corrected) (W. Giggenbach, personal communication). The factor of 2 is the approximate value of the $N_2 \pm O_2$ ratio in air-saturated water.

5.4. Redox potential

In addition to the sampling for chemical analyses, we also sampled a limited amount of water from each vent during a single dive for simultaneous on-board Eh and pH measurements in order to assess if there is a significant redox difference between the individual vent fluids. The pH measurement was used to monitor seawater contamination and the quality of the Eh measurement was checked against the Quinhydrone solution (e.g., Clark and Fritz, 1997). All vent fluids were found to be reducing and have similar Eh values; vent 1 = −0.175 V, vent 2 = −0.171 V, vent 3 = −0.173 V and vent 4 = −0.175 V. These values are similar to those obtained from As^{3+}/As^{5+} calculations (Fig. 11).

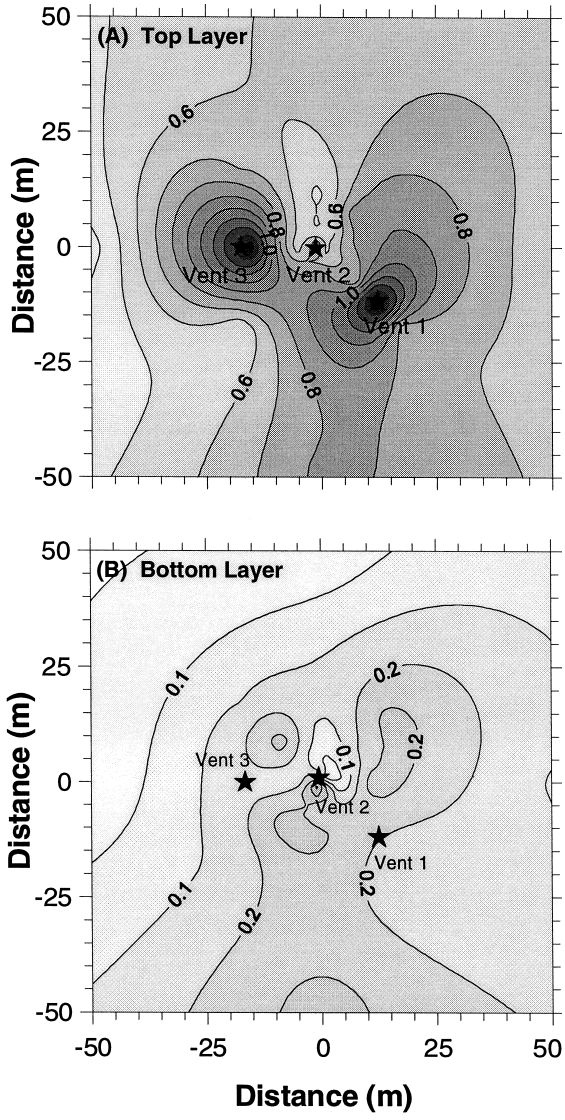

Fig. 12. Model of hydrothermal component in (A) surface and (B) bottom water in Tutum Bay. The contour lines were calculated with Eq. (2) (see text) and represent the concentration of hydrothermal component in %. The darker colors indicate higher hydrothermal component.

6. Hydrothermal fluid dissipation and its effect on Tutum Bay seawater

The contour maps of the hydrothermal component concentration in Tutum Bay seawater (Figs. 12 and 13) were constructed using silica as a tracer and assuming conservative behavior and linear mixing. Relative to seawater, silica showed the highest concentration in the hydrothermal fluids (Table 1). The hydrothermal component in Tutum Bay seawater was calculated using a simple mass balance equation:

$$C_{TBW} = xC_{SW} + yC_{HF} \quad (2)$$

where C_{TBW} is the silica concentration in Tutum Bay seawater, C_{SW} is the silica concentration in reference seawater and C_{HF} is the silica concentration in the hydrothermal fluid.

The bottom water in Tutum Bay shows varying degrees of hydrothermal component and values range from 0.05 and 0.30% (Fig. 12). The small area just below vent 2 shows the highest concentrations, but this is an area where hydrothermal fluids seep through the sandy bottom at very low discharge rates. The low concentrations of hydrothermal fluid in the bottom water are not surprising given the physico-chemical conditions of fluid discharge. The vent fluids have a salinity of $< 3½$, which combined with their discharge temperature of $\sim 90°C$, makes them buoyant relative to seawater. As a result the hydrothermal fluids quickly rise to the surface (Fig. 3) and the surface water shows an up to 10 times higher hydrothermal component concentration than the bottom water (Fig. 12). Only little mixing occurs with ambient seawater in the immediate proximity of vent orifices. The overall distribution of hydrothermal component is most likely controlled by two processes: (1) diffuse low rate discharge of hydrothermal fluid and (2) the development of hy-

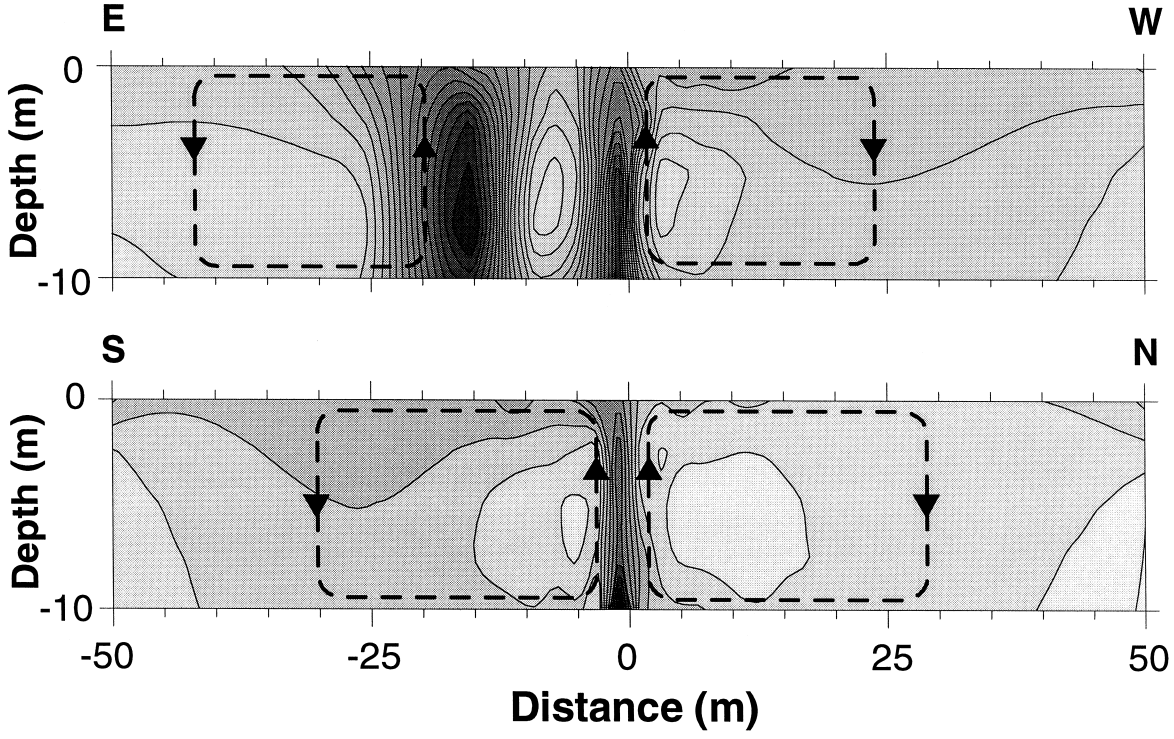

Fig. 13. Cross-section model of hydrothermal component in Tutum Bay. The contour lines were calculated with Eq. (2) (see text) and represent the concentration of hydrothermal component. The darker colors indicate higher hydrothermal component. Suggested hydrothermal convection cells are indicated by dashed lines.

drothermal convection cells within the bay due to temperature differences (Fig. 13).

It is important, however, to realize that the fluid dissipation model presented in Figs. 12 and 13 is only a snapshot in space and time of a very dynamic system. At times discharge rates may be much higher or lower resulting in a different concentration of hydrothermal component. Nearshore currents, although none were noticed while sampling, may be present at other times, modifying the plume dispersion pattern.

Of potentially poisonous trace metals that are released into Tutum Bay, only arsenic has a significantly higher concentration than seawater. In particular, AsIII-compounds are known to have a genotoxic potential (Gebel et al., 1997). The hydrothermal fluids contain extremely high arsenic concentrations of more than 11 μmol and the combined discharge of all vents is estimated to be more than 1500 g of arsenic per day into an area of approximately 50 m by 100 m with an average depth of 6 m. These values are the highest arsenic concentration reported from any marine setting, including black smoker fluids from mid-ocean ridges. Despite the amount of arsenic released into the bay, corals, clams and fish do not show any direct response to the elevated values. Fish have been observed to hover over vent orifices, bathing in the hydrothermal fluid. The diversity and health of the coral reef is indiscernible from reefs that are not exposed to hydrothermal discharge. Pichler et al. (for submission) analyzed the skeletons of scleractinian corals and the shells of *Tridacna gigas* clams but they did not find elevated concentrations of arsenic or other trace metals when compared to specimens collected from outside Tutum Bay.

Two mechanisms efficiently control and buffer the arsenic concentration: (1) dilution by seawater and (2) incorporation in and adsorption on Fe-oxyhydroxides that precipitate when the hydrothermal fluids mix with ambient seawater. The hydrothermal fluids have a pH of ~ 6 and are slightly reducing. Under these conditions Mn stays in its reduced form and, therefore, in solution, whereas As is rapidly oxidized and scavenged by Fe-oxyhydroxides. Oxidation of As^{3+} to its pentavalent state significantly decreases its reactivity and genotoxicity (Gebel et al., 1997). The Fe-oxyhydroxides that precipitate in Tutum Bay can contain more than 50 000 ppm As (Pichler and Dix, 1996; Pichler et al., 1996) and are by an order of magnitude the highest As values found in a natural system.

7. Discussion

The discharge composition of thermal springs is controlled by two sets of processes: (1) deep reservoir conditions (deep reservoir = reaction zone immediately above the heat source), and (2) secondary processes during ascent. In the deep reservoir, host rock composition, temperature, direct magmatic contributions and residence time are the controlling factors. During ascent, a drop in pressure and temperature can initiate phase separation and mineral precipitation, causing a dramatic change in fluid composition. Mixing with other hydrothermal fluids and/or groundwater is possible at any depth. In near-shore and submarine environments, mixing with seawater cannot be ruled out. The chemical composition of a hydrothermal fluid, sampled at the surface, generally contains an imprint of its subsurface history. Chemically inert constituents (tracers) provide information about their source, whereas chemically reactive species (geoindicators) record physicochemical changes (e.g., Ellis and Mahon, 1977; Giggenbach, 1991; Nicholson, 1992). Examples of widely used solute tracers and geoindicators are Cl, B, Li, Rb, Cs and Na, K, Mg, Ca, SiO_2, respectively. The boundary between the two groups, however, is not rigid and depending on the physicochemical conditions of the hydrothermal system, tracers may participate in chemical reactions and geoindicators can behave inertly.

In Tutum Bay waters, the ratios of all alkalis, except for Li, are almost identical to those in samples W-1 and W-2. This would argue that at least some of the relative Li increase has to be attributed to shallow leaching, a proposition contrary to the belief that Li is the alkali probably least affected by secondary processes (e.g., Giggenbach, 1991). These elements are added to the hydrothermal fluid under deep reservoir conditions due to water±rock interaction and they are generally not affected by shallow processes. All samples plot away from the compositional field of crustal rocks, indicating that secondary

processes must have affected their composition. The crystallization of illite at high temperature has removed some of the initial Rb from fluids W-1 and W-2 (Fig. 14). The Li/Cs ratios are dependent on lithology and the intermediate position between basalt and rhyolite of W-1 and W-2 is in good agreement with the andesitic composition of the Ambitle volcano (Wallace et al., 1983). The relatively higher Li content of the Tutum Bay fluids may be a result of Li-uptake due to shallow processes or mixing with meteoric water (Fig. 14). The loss of Cs to zeolites is most likely not of any importance considering that the Rb/Cs ratios in Tutum Bay and on-shore samples (W-1 and W-2) more or less remain constant.

The REE patterns (Fig. 10) are as expected for hydrothermal fluids with a pH of ~6 (Michard, 1989). The pattern geometry is similar to that of the host rocks (Fig. 10) but Ce, Pr, Nd and Sm are relatively depleted which reflects their greater immobility during hydrothermal alteration (Thompson, 1991). Some of the Ce may also have been lost due to adsorption onto or co-precipitation with Fe-oxyhydroxides prior to sampling. Ce^{3+} is easily oxidized to Ce^{4+} and may directly precipitate as CeO_2 while the other REEs still remain in their trivalent state (Goldberg et al., 1963). In addition, Ce forms colloidal ceric hydroxide (Carpenter and Grant, 1967) which is readily scavenged by Fe-oxyhydroxides. The slight difference in pattern geometry between area A and B could be caused as well by varying degrees of subsurface mixing. This, however, does not account for the difference in vent 2 samples.

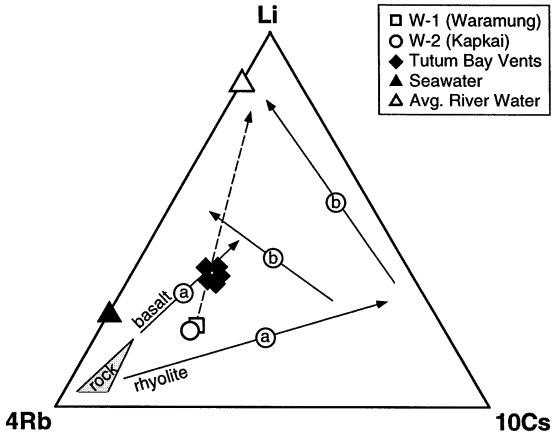

Fig. 14. Relative Li, Rb and Cs contents of Tutum Bay, Waramung and Kapkai hot-springs. The two arrows (a) indicate fluid evolution due to Rb-uptake during precipitation of illite at $t >$ 300°C and the two arrows (b) indicate fluid evolution due to Cs-uptake during precipitation of zeolites at $t <$ 300°C. The dashed line indicates the relative Li uptake by the hydrothermal fluid due to shallow processes (see text) and possible entrainment of meteoric water.

7.1. Origin of the hydrothermal fluid and probable mixing trends

A fluid in a hydrothermal system may be derived from any or any combination of the following sources: meteoric water, seawater, connate water, magmatic water and juvenile water. Mixing of waters from different sources affects many aspects of the geochemistry of a hydrothermal system, such as chemical composition, isotopic composition, temperature profile and gas content. Deep sea hydrothermal systems active along mid-oceanic ridges, in back-arc basins and on the flanks of seamounts likely derive all their fluid from seawater, although a minor magmatic contribution cannot be completely ruled out (De Ronde, 1995). In contrast, on-land hydrothermal areas derive most of their fluid from meteoric sources, but a significant magmatic contribution is likely (e.g., Giggenbach, 1992). Determination of the fluid origin is an important step in order to determine subsurface processes and reservoir conditions. While the source determination is relatively straightforward in deep marine and inland settings, the subject becomes more complex in coastal regions (off-shore and on-shore) where seawater incursion can significantly alter the fluid composition in a hydrothermal system. For example, seawater mixing is present in the Savusava (Fiji), Puna (Hawaii) and Reykjanes (Iceland) hydrothermal systems (Nicholson, 1992). Similarly, meteoric water may be the source for submarine hydrothermal systems in coastal areas where a steep topography and ample supply of rainwater can force the Ghyben±Herzberg (freshwater± seawater) boundary substantially offshore (Nahm, 1966; Chuck, 1967). Tropical and subtropical island-arc volcanoes are good examples for these conditions. Subsurface sealing of a hydrothermal system, as argued for White Island, New Zealand (Giggen-

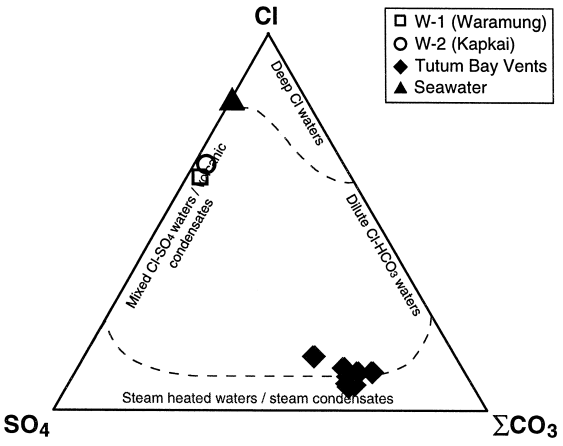

Fig. 15. Relative Cl, SO_4 and ∑CO3 contents of Tutum Bay, Waramung and Kapkai hot-springs. Empty symbols indicate SO_4 corrected position (see text). ΣCO_3 has been corrected for seawater contamination and includes H_2CO_3 and HCO_3.

bach et al., 1989), can be another mechanism to prevent seawater from entering the nearshore environment, thus allowing for a meteoric water dominated submarine hydrothermal system.

The hydrothermal fluids in Tutum Bay, although discharging in a submarine environment, are most likely derived from a meteoric source. Total dissolved solids (TDS) are rather low (< 3000 mg/l) and molecular ratios indicative of seawater dilution, such as Cl/Mg, Cl/Br, Cl/SO_4 and Ca/Mg (Nicholson, 1992), are quite different from those caused by seawater mixing. Their origin and physicochemical history can be explored in a Cl, SO_4 and HCO_3 ternary diagram (e.g., Chang, 1984; Giggenbach, 1991; Nicholson, 1992; Giggenbach, 1997). Hydrothermal waters are generally divided into neutral chloride, acid sulfate and bicarbonate waters, but mixtures between the individual groups are common (Fig. 15). Tutum Bay vents plot close to the ΣCO_3 corner along the upper boundary for steam heated waters. Waters that plot in this area generally form by underground absorption of vapors separated from a deeper neutral chloride water into cooler ground water, where based on the gas content of the vapor and redox conditions either acid sulfate or bicarbonate waters are formed (e.g., Ellis and Mahon, 1977; Henley and Ellis, 1983; Hedenquist, 1990; Giggenbach, 1997). The relatively high SO_4^{2-} content can be attributed to oxidation of H_2S, thus shifting the samples away from their original field along the Cl±ΣCO_3 mixing line (Fig. 15).

Two other elements, Cl and B, are widely used to trace the origin and subsurface flow direction of hydrothermal fluids (e.g., Nicholson, 1992). In the case of the Tutum Bay samples, however, Cl cannot be applied successfully because the concentration gradient between seawater and hydrothermal fluid is too large and, therefore, the error introduced due to seawater contamination is substantial. Boron, on the other hand, seems to be an excellent tracer for subsurface conditions at Ambitle Island. The subsurface flow direction from W-2 over W-1 to Tutum Bay is indicated by decreasing B and alkali contents (Fig. 16) which record dilution of the deep reservoir fluid by either groundwater or bicarbonate water. This is in accord with their geographic and topo-

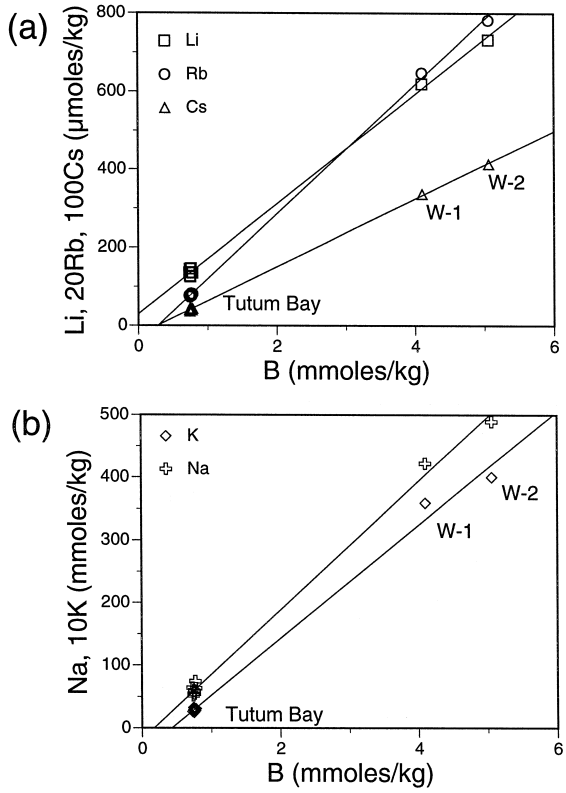

Fig. 16. (a) Li, Rb and Cs vs. B in Tutum Bay, Waramung (W-1) and Kapkai (W-2) hot-springs. $r^2 > 0.99$ for all linear regression lines. (b) Na and K vs. B in Tutum Bay, Waramung (W-1) and Kapkai (W-2) hot-springs. $r^2 > 0.91$ for all linear regression lines.

graphic location. The Tutum Bay vents are topographically lowest and furthest away from the center of the hydrothermal system, whereas the sample from the Kapkai thermal area (W-2) is relatively higher (approximately 30 m above sea level) and closer. The linear regression lines for Rb and Cs and for Na and K converge almost exactly at the point where they intercept the *x*-axis (Fig. 16). Assuming that the regression lines represent mixing between deep neutral chloride and shallow bicarbonate water, the intercept of the *x*- or *y*-axis represents one endmember. This endmember, if based on Rb and Cs, would have a boron excess, of approximately 0.27 mmol, whereas the one based on Li would have a Li excess of approximately 0.04 mmol (Fig. 16). The former is a much more likely alternative for a process that forms bicarbonate water. Boron occurs largely as boric acid (H_3BO_3), its volatile form, and can be easily carried in the vapor phase even at lower temperatures (Tonani, 1970). Using a simple mass balance equation:

$$C_{TBVF} = xC_{DR} + yC_{BW} \quad (3)$$

where C_{TBVF} is the average boron concentration in Tutum Bay vent fluids, C_{DR} is the estimated boron concentration in the deep reservoir fluid and C_{BW} is the calculated boron concentration in the bicarbonate water. Based on the 0.27 mmol boron excess, bicarbonate and chloride water fractions were calculated to be 0.89 and 0.11, respectively. Based on the Na±K boron excess, bicarbonate and chloride water fractions would be approximately 0.93 and 0.07, respectively. The deep reservoir fraction, present in Tutum Bay samples, is in good agreement with that found in waters of similar origin in other hydrothermal systems. Hedenquist (1990), for example, estimated that at the Broadlands±Ohaaki geothermal system, most of the marginal upflow mixes with steam-heated waters and only a small amount of deep fluid (~ 10%) rises to the surface.

The division into area A and B that was initially based solely on geographic location has been reinforced by chemical composition. Although the chemical composition of all Tutum Bay vents is quite alike, compared to area A, area B vents have higher K, Rb, Sb, Cs, Tl, and As and lower Ca, Li, Mn, Fe, and Sr concentrations (Table 2). This seems to be directly related to the composition of samples W-1 and W-2 that also have elevated concentrations of K, Rb, Sb, Cs, Tl, and As and lower Ca, Li, Mn, Fe, and Sr concentrations (Tables 1 and 2). Thus the slight chemical difference in area A and B vents may be attributed to varying subsurface addition of a hydrothermal fluid similar in composition to W-1 and W-2.

7.2. Geothermometry

Solute geothermometers, such as listed in Table 4, provide powerful tools to estimate subsurface conditions. Their successful application has been extensively discussed in the geothermal literature and relies on five basic assumptions: (1) exclusively temperature dependent mineral±fluid reaction; (2) abundance of the mineral and/or solute; (3) chemical equilibrium; (4) no re-equilibration; and (5) no mixing or dilution (Nicholson, 1992). The no mixing or dilution assumption, however, can be circumvented if their extent and/or influence on solute ratios (e.g., Na/K) is known (see above).

The calculated temperatures in Table 4 differ quite drastically. This is not surprising considering that most problems in the use of geothermometers arise from application to unsuitable samples. Different geothermometers, however, record different equilibria and disagreement does not immediately eliminate the use of one or the other. Careful application and evaluation of calculated temperatures may provide important clues to the overall hydrology of the hydrothermal system.

The temperatures calculated with the silica geothermometers (Fournier, 1977) are too low to represent a reliable estimate of the reservoir condition. This is to be expected in particular for the samples W-1 and W-2, since these springs are fed from reservoirs with temperatures in excess of ~ 230°C and have, therefore, lost some of their initial silica due to precipitation of quartz, chalcedony, or amorphous silica during ascent (Rimstidt and Barnes, 1980; Fournier, 1985). The application of the silica thermometer to Tutum Bay samples (V-1 to V-4) is problematic because they are a mixture of at least two fluids and the thermometer is based on absolute silica concentration.

The quality of reservoir temperatures calculated with the thermometers listed in Table 4 depends

Table 4
Calculated reservoir temperatures for Kapkai, Waramung and Tutum Bay vent fluids

Thermometer	T (°C)						Reference
	Vent 1	Vent 2	Vent 3	Vent 4	W-1	W-2	
Amorphous silica	9	8	8	7	−3	6	Fournier (1977)
Chalcedony	100	99	99	98	86	97	Fournier (1977)
Quartz	128	127	127	126	114	125	Fournier (1977)
Quartz steam loss	125	124	124	123	113	122	Fournier (1977)
K/Mg	n.d.	n.d.	n.d.	n.d.	306	310	Giggenbach (1988)
Li/Mg	n.d.	n.d.	n.d.	n.d.	203	209	Kharaka and Mariner (1989)
Na/Li	166	172	169	168	111	112	Kharaka and Lico (1982)
Na/K	246	253	252	273	276	271	Fournier (1979)
Na/K	240	245	244	262	264	260	Giggenbach (1988)
Na±K±Ca	191	192	192	206	312	320	Fournier and Truesdell (1973)

strongly on the equilibrium between fluid and host rock lithology. Attainment of deep reservoir equilibrium has been verified for samples W-1 and W-2 based on their relative Na, K and Mg concentrations (e.g., Giggenbach, 1988). Unfortunately, this method cannot be directly applied to the Tutum Bay samples because they have zero-Mg by definition, but equilibrium conditions would apply for Mg concentrations between approximately 0.00083 and 0.083 mmol. Temperatures obtained from the Li/Mg and Na/Li thermometers are substantially lower than those from the other ionic solute thermometers (Table 4). Exchange reactions with Mg seem to be expeditious at lower temperatures and Mg-based thermometers may, therefore, record the last equilibrium prior to discharge (e.g., Nicholson, 1992). The low Li/Mg temperature, however, is in contrast with the K/Mg thermometer. Considering that the relative Mg, Na and K concentrations of W-1 and W-2 indicate deep reservoir equilibrium, it is rather the Li concentration that must have been affected during ascent or at a shallower level. The temperatures obtained from K/Mg, Na/K and Na±K±Ca are in good agreement and indicate a reservoir temperature of approximately 300°C. Na/K temperatures are slightly lower, which is to be expected given the slightly peripheral location of the thermal areas. The Na/K ratio of a hydrothermal fluid generally increases during lateral flow (Ellis and Mahon, 1977). The Tutum Bay samples, although mixed with water of a different origin, still carry a significant Na/K imprint of the deep reservoir. Temperatures for vents 1, 2 and 3 are slightly lower, while vent 4 has identical temperatures to W-1 and W-2 (Table 4). This would confirm that the discharge from vent 4 has a relatively greater proportion of the deep reservoir fluid (see above). The notable disagreement between Tutum Bay and on-land Na±K±Ca temperatures is a result of the high pCO_2 and, therefore, high Ca concentration in Tutum Bay fluids.

The Na/Li temperatures obtained for Tutum Bay samples may be representative of shallow reservoir conditions that post date mixing between deep reservoir and bicarbonate fluid. When compared to Mg, Na, K, Rb and Cs, Li seems to be the element most affected by shallow reservoir processes, but the calculated Na/Li temperatures appear to be in good agreement with theoretical considerations. Let us consider one more time the process that leads to the formation of a CO_2 or bicarbonate water. Isenthalpic expansion of steam, separated from a deeper liquid phase to close to atmospheric pressure, is accompanied by a drop in temperature to about 160°C (Giggenbach, 1997). Bicarbonate waters formed due to interaction between groundwater and this 160°C steam, generally have temperatures in the vicinity of 150°C (e.g., Cioni and D'Amore, 1984; Hedenquist, 1990). Mixing of this 150°C bicarbonate water with a 300°C deep reservoir fluid at a ratio of ~9:1, as obtained from the boron mixing model (see above), leads to a final shallow reservoir temperature of 165°C which is in perfect agreement with the calculated Na/Li temperatures (Table 4).

Additional insight into potential processes controlling the fluid composition and subsurface processes may be provided by the chemical composition of the

gases, as listed in Table 3. An examination of the gases is carried out in terms of relative concentrations of N_2(c), He and CO_2 contents. On the basis of gas discharges from a wide range of tectonic environments, the compositions of volcanic and geothermal vapors were found to represent essentially mixtures of two endmember components: a mantle derived component, very low in N_2 with CO_2/He ratios of 20 000 to 40 000, and an arc-type component with much higher CO_2/He ratios of $> 10^6$ and a quite uniform CO_2/N_2 ratios of 100 ± 60 (Giggenbach, 1995).

The data points for the gases plot at the upper boundary of the compositional area outlined for volcanic and geothermal vapors (Fig. 17) and across the middle of the triangle, suggesting a major input of mantle-derived gases. The increased relative N_2 contents may reflect increased stripping of N_2 during the rise of the gases through air-saturated seawater or groundwater. Increased interaction of the gases with water can be expected to lead to removal of soluble components, an assumption supported by the absence of H_2S, the most soluble component (Table 3) which leads to the higher SO_4/Cl in Tutum Bay vent fluids when compared to samples W-1 and W-2.

Assuming equilibration of the gases dissolved in a liquid phase and preservation of equilibrium

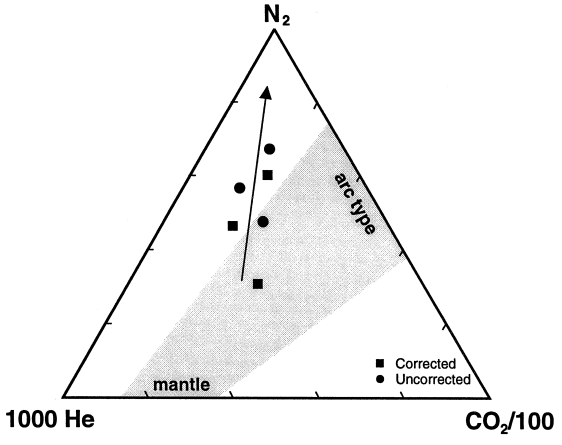

Fig. 17. Relative CO_2, N_2 and He contents of non-condensable gases collected from submarine discharges in Tutum Bay. The shaded area indicates the relative position for mantle and arc type gases. The arrow indicates N_2 uptake due to sample contamination with air.

CH_4/CO_2 ratios in the samples (Giggenbach and Matsuo, 1991), the $CH_4 \pm CO_2$ equilibrium temperatures are between 257 and 291°C (Table 3). Depth of separation, therefore, should be at approximately 1000 m, provided that the deep reservoir fluid is on the boiling curve. These $CH_4 \pm CO_2$ equilibrium temperatures are in good agreement with reservoir fluid estimates based on the Mg/Li, Na/K and Na±K±Ca solute geothermometers (Table 4).

8. Summary and conclusions

The shallow-water hydrothermal fluids from Tutum Bay seem to be dominantly of meteoric origin, although they discharge in a marine environment. This confirms the work of Pichler and Dix (1996) who, based on fluid inclusions and $\delta^{18}O$ in hydrothermal aragonite, also proposed their meteoric origin. Their final chemical composition is the outcome of a two- or possibly three-step process (Fig. 18): (1) Phase separation in the deep reservoir beneath Ambitle Island produces a high temperature vapor that rises upward and subsequently reacts with cooler ground water to form a low pH, CO_2-rich water of approximately 150±160°C. This fluid is highly reactive and pH±Eh sensitive elements such as Fe, Mn, Ca and Sr are leached from the host rock in the shallow reservoir. (2) Due to the steep topography, this CO_2-rich fluid moves laterally towards the margin of the hydrothermal system where it mixes with the marginal upflow of the deep reservoir fluid. This produces a dilute chloride water of approximately 165°C. A third step may be the entrainment of minor amounts of ground or seawater during its final ascent. Based on a B±Rb/Cs mixing model, it has been estimated that approximately 10% of the deep reservoir fluid reaches the surface.

The definite chemical composition of Tutum Bay vent fluids may be slightly different from the values reported in Table 2, because of phase separation during ascent from the shallow reservoir and Mg-correction for seawater contamination. Thermometry and mixing calculations, however, are not affected, because they are based on element ratios rather than on absolute concentrations.

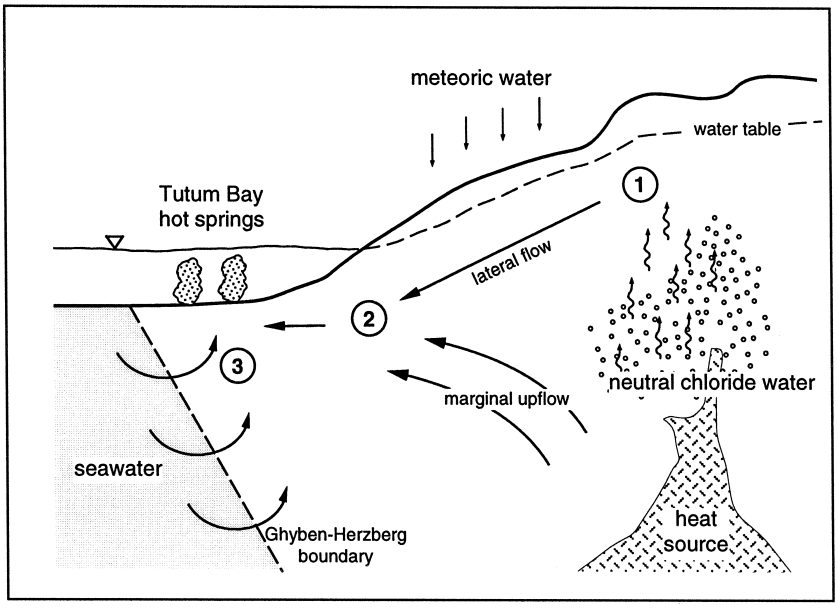

Fig. 18. Hypothetical cross section through Tutum Bay and the west side of Ambitle Island. The circled numbers (1, 2 and 3) indicate the approximate location of subsurface reaction zones: (1) Formation of a steam heated bicarbonate water, (2) gravity driven lateral flow and mixing with marginal upflow from deep reservoir neutral chloride water, and (3) possible mixing with seawater near the Ghyben±Herzberg boundary.

Compared to seawater, the hydrothermal fluids are depleted in Cl, Br, SO_4, Na, K, Ca, Mg, and Sr and enriched in HCO_3, B, Si, Li, Mn, Fe, Rb, Cs, Sb, Tl, and As. Although some elements are significantly enriched, they do not have a clear impact on ambient seawater composition because their concentration is buffered by mixing and uptake into secondary minerals. Only the surface water in Tutum Bay carries a clear imprint of the hydrothermal fluids.

Acknowledgements

Most of this research was funded by an American Chemical Society, Petroleum Research Grant (No. 31585-AC8) and Natural Sciences and Engineering Research Council of Canada operating grant to Jan Veizer. Thomas Pichler acknowledges the support of two Geological Society of America Student Research Grants (Nos. 5681-95 and 5904-96). We all would like to thank John Loop, Judy Vaive and Jean Pelchat for help with the water analyses. Thomas Pichler is grateful to Donna Switzer and Yannick Beaudoin for help underwater, to Ajaz Karim and Johannes Barth for sharing their thoughts on water sampling and to Werner Giggenbach for the gas analyses. We wish to thank Drs. David Butterfield and Paul Dando for their constructive reviews. An earlier version of this paper benefited from comments by Ian Clark.

References

Bishoff, J.L., Dickson, F.W., 1975. Seawater basalt interaction at 200°C and 500 bars: implications for the origin of seafloor heavy metal deposits and the regulations of seawater chemistry. Earth and Planetary Science Letters 25, 385±397.

Brookins, D.G., 1988. E_h±pH Diagrams for Geochemistry. Springer-Verlag, New York, 178 pp.

Butterfield, D.A., Massoth, G.J., McDuff, R.E., Lupton, J.E., Lilley, M.D., 1990. Geochemistry of hydrothermal fluids from Axial Seamount hydrothermal emissions study vent field, Juan de Fuca Ridge: subseafloor boiling and subsequent fluid±rock interaction. Journal of Geophysical Research 95 (B8), 12895± 12921.

Carpenter, J.H., Grant, V.E., 1967. Concentration and state of cerium in coastal waters. Journal of Marine Research 25, 228±238.

Chang, C.L., 1984. Triangular diagrams for predication of aquifer chemistry. Geothermal Research Council Transactions 8, 373±376.

Chuck, R.T., 1967. Groundwater resources development on tropical islands of volcanic origin. Int. Conf. Water for Peace, Washington, DC, pp. 963±970.

Cioni, R., D'Amore, F., 1984. A genetic model for the crater fumaroles of Vulcano Island (Sicily, Italy). Geothermics 13 (4), 375±384.

Clark, I.D., Fritz, P., 1997. Environmental isotopes in hydrogeology. Lewis Publishers, Boca Raton, 328 pp.

Dando, P.R., Leahy, Y., 1993. Hydrothermal activity off Milos, Hellenic Volcanic Arc. Bridge News 20±21.

Davies, R.M., Ballantyne, G.H., 1987. Geology of the Ladolam gold deposit Lihir Island, Papua New Guinea. Pacific Rim Congress 87. Australasian Institute of Mining and Metallurgy, Gold Coast, Australia, pp. 943±949.

De Ronde, C.E.J., 1995. Fluid chemistry and isotopic characteristics of seafloor hydrothermal systems and associated VMS deposits: potential for magmatic contributions. In: Thompson, J.F.H. (Ed.), Magmas, Fluids, and Ore Deposits. Mineralogical Association of Canada Short Course Series. Mineralogical Association of Canada, Victoria, pp. 479±509.

Driehaus, W., Jekel, M., 1992. Determination of As(III) and total inorganic arsenic by on-line pretreatment in hydride generation atomic absorption spectrometry. Fresenius Journal of Analytical Chemistry 343, 352±356.

Ellis, A.J., Mahon, W.A.J., 1977. Chemistry and Geothermal Systems. Academic Press, New York, 392 pp.

Fleet, A.J., 1984. Aqueous and sedimentary geochemistry of the rare earth elements. In: Henderson, P. (Ed.), Rare Earth Element Geochemistry. Developments in Geochemistry. Elsevier, pp. 343±373.

Fournier, R.O., 1977. Chemical geothermometers and mixing models for geothermal systems. Geothermics 5, 41±50.

Fournier, R.O., 1979. A revised equation for the Na/K geothermometer. Geothermal Research Council Transactions 3, 221±224.

Fournier, R.O., 1985. The behavior of silica in hydrothermal solutions. In: Berger, B.R., Bethke, P.M. (Eds.), Geology and Geochemistry of Epithermal Systems. Economic Geology, pp. 45±61.

Fournier, R.O., Truesdell, A.H., 1973. An empirical Na±K±Ca geothermometer for natural waters. Geochimica et Cosmochimica Acta 37, 1255±1275.

Gebel, T., Christensen, S., Dunkelberg, H., 1997. Comparative and environmental genotoxicity of antimony and arsenic. Anticancer Research 17, 2603±2607.

Giggenbach, W., 1988. Geothermal solute equilibria. Derivation of Na±K±Mg±Ca geoindicators. Geochimica et Cosmochimica Acta 52, 2749±2765.

Giggenbach, W.F., 1991. Chemical techniques in geothermal exploration. In: D'Amore, F. (Ed.), Application of geochemistry in geothermal reservoir development. UNITAR/UNDP, Rome, pp. 252±270.

Giggenbach, W.F., 1992. Isotopic shifts in waters from geothermal and volcanic systems along convergent plate boundaries and thier origin. Earth and Planetary Science Letters 113, 495±510.

Giggenbach, W.F., 1995. Composition of fluids in geothermal systems of the Taupo Volcanic Zone, New Zealand, as a function of source magma. International Symposium Water±Rock Interaction, Vladivostok, pp. 9±12.

Giggenbach, W.F., 1997. The origin and evolution of fluids in magmatic±hydrothermal systems. In: Barnes, H.L. (Ed.), Geochemistry of Hydrothermal Ore Deposits. Wiley, New York, pp. 737±796.

Giggenbach, W.F., Goguel, R.L., 1989. Collection and analysis of geothermal and volcanic water and gas discharges. NZ DSIR, 2401.

Giggenbach, W.F., Matsuo, S., 1991. Evaluation of results from second and third IAVCEI Field Workshops on Volcanic Gases, Mt. Usu, Japan, and White Island, New Zealand. Applied Geochemistry 6, 125±141.

Giggenbach, W.F., Hedenquist, J.W., Houghton, B.F., Otway, P.M., Allis, R.G., 1989. Research drilling into the volcanic hydrothermal system on White Island, New Zealand. EOS (Transactions, American Geophysical Union) 70, 98±109.

Goldberg, E.D., Koide, M., Schmitt, R.A., Smith, R.H., 1963. Rare earth distributions in the marine environment. Journal of Geophysical Research 68, 4209±4217.

HACH, 1992. Digital titrator model 16900-01 manual. Loveland, CO, 47 pp.

Hall, G.E.M., Vaive, J.E., McConnell, J.W., 1995. Development and application of a sensitive and rapid analytical method to determine the rare-earth elements in surface waters. Chemical Geology 120, 91±109.

Hall, G.E.M., Vaive, J.E., Pelchat, J.C., 1996. Performance of inductively coupled plasma mass spectrometric methods used in determination of trace elements in surface waters in hydrogeochemical surveys. Journal of Analytical Atomic Spectrometry 11, 779±786.

Haskin, L.A., Haskin, M.A., Frey, F.A., Wildman, T.R., 1968. Relative and absolute terrstrial abundance of the rare earths. In: Ahrens, L.H. (Ed.), Origin and Distribution of the Elements. Pergamon, Oxford, pp. 889±911.

Hedenquist, J.W., 1990. The thermal and geochemical structure of the Broadlands±Ohaaki geothermal system, New Zealand. Geothermics 19, 151±185.

Heikoop, J.M., Tsujita, C.J., Risk, M.J., Tomascik, T., Mah, A.J., 1996. Modern iron ooids from a shallow-marine volcanic setting: Magengetang, Indonesia. Geology 24 (8), 759±762.

Henley, R.W., Ellis, A.J., 1983. Geothermal systems ancient and modern: a geothermical review. Earth-Science Reviews 19, 1±50.

Henley, R.W., Truesdell, A.H., Barton, P.B.J., 1984. Fluid±mineral equilibria in hydrothermal systems. In: Reviews in Economic Geology, 1. Society of Economic Geologists, 267 pp.

Hodkinson, R.A., Cronan, D.S., Varnavas, S., Perissoratis, C., 1994. Regional geochemistry of sediments from the Hellenic Volcani Arc in regard to submarine hydrothermal activity. Marine Georesources and Geotechnology 12, 83±129.

Kharaka, Y.K., Lico, M.S., 1982. Chemical geothermometers

applied to formation waters, Gulf of Mexico and California basins. AAPG Bulletin 66, 588±598.
Kharaka, Y.K., Mariner, R.H., 1989. Chemical geothermometers and their application to formation waters from sedimentary basins. In: Naeser, N.D., McCulloch, T.H. (Eds.), Thermal History of Sedimentary Basins: Methods and Case Histories. Springer-Verlag, New York, pp. 99±117.
Licence, P.S., Terrill, J.E., Fergusson, L.J., 1987. Epithermal gold mineralization, Ambitle Island, Papua New Guinea. Pacific Rim Congress '87. Australasian Institute of Mining and Metallurgy, Gold Coast, Queensland, pp. 273±278.
McInnes, B.I.A., Cameron, E.M., 1994. Carbonated, alkaline metasomatic melts from a sub-arc environment: mantle wedge samples from the Tabar±Lihir±Tanga±Feni arc, Papua New Guinea. Earth and Planetary Science Letters 122, 125±141.
Michard, A., 1989. Rare earth element systematics in hydrothermal fluids. Geochimica et Cosmochimica Acta 53, 745±750.
Nahm, G.-Y., 1966. Geology and groundwater resources of volcanic island, Cheju-do. Geology and Ground-Water Resources 3, 109±133.
Nicholson, K., 1992. Geothermal Fluids. Springer-Verlag, 266 pp.
O'Hara, S.C.M., Dando, P.R., Schuster, U., Bennis, A., Boyle, J.D., Chui, F.T.W., Hatherell, T.V.J., Niven, S.J., Taylor, L.J., 1994. Gas seep induced water interstitial water circulation: observations and environmental implications. Continental Shelf Research 15, 931±948.
Pichler, T., Dix, G.R., 1996. Hydrothermal venting within a coral reef ecosystem, Ambitle Island, Papua New Guinea. Geology 20 (5), 435±438.
Pichler, T., Hannington, M.D., McInnes, B.I.A., Watkinson, D.H., Staff, K.A.L.M.C., 1995. Shallow submarine venting in the Tabar±Feni Arc: mineralogy and geochemistry of hydrothermal precipitates. Geological Association of Canada/Mineralogical Association of Canada Annual Meeting, Victoria, British Columbia, p. A-83.
Pichler, T., Veizer, J., Hall, G.E.M., 1996. Unusual aragonite and As-rich Fe-oxyhydroxide precipitates from a shallow-water submarine hydrothermal system, Ambitle Island, Papua New Guinea. Geological Society of America Annual Meeting, Denver.
Rimstidt, J.D., Barnes, H.L., 1980. The kinetics of silica±water reactions. Geochimica et Cosmochimica Acta 44, 1683±1699.
Sarano, F., Murphy, R.C., Houghton, B.F., Hedenquist, J.W., 1989. Preliminary observations of submarine geothermal activity in the vicinity of White Island Volcano, Taupo Volcanic Zone, New Zealand. Journal of the Royal Society of New Zealand 4, 449±459.
Sedwick, P., Stüben, D., 1996. Chemistry of shallow submarine warm springs in an arc±volcanic setting: Vulcano Island, Aeolian Archipelago, Italy. Marine Chemistry 53, 146±161.
Swan, A.R.H., Sandilands, M., 1995. Introduction to Geological Data Analysis. Blackwell Science, Oxford, 446 pp.
Thompson, G., 1991. Metamorphic and hydrothermal processes: basalt±seawater interactions. In: Floyd, P.A. (Ed.), Oceanic Basalts. Blackie, Glasgow, pp. 148±173.
Tonani, F., 1970. Geochemical methods of exploration for geothermal energy. Geothermics 2, 492±515.
Varnavas, S.P., Cronan, D.S., 1991. Hydrothermal metallogenic processes off the islands of Nisiros and Kos in the Hellenic Volcanic Arc. Marine Geology 99, 109±133.
Vidal, M.V., Vidal, F.V., Isaacs, J.D., Young, D.R., 1978. Coastal submarine hydrothermal activity off northern Baja California. Journal of Geophysical Research 83 (B4), 1757±1774.
Vidal, M.V., Vidal, F.V., Isaacs, J.D., 1981. Coastal submarine hydrothermal activity off northern Baja California: 2. Evolutionary history and isotope geochemistry. Journal of Geophysical Research 86 (B10), 9451±9468.
Wallace, D.A., et al., 1983. Cainozoic volcanism of the Tabar, Lihir, Tanga, and Feni islands, Papua New Guinea: geology, whole-rock analyses, and rock-forming mineral compositions. 243, Bureau of Mineral Resources Geology and Geophysics.